The Exact Ground State of the Frenkel-Kontorova Model with Repeated Parabolic Potential
II. Numerical Treatment

T. Scheidsteger
Hochschulrechenzentrum
Technische Hochschule Darmstadt
Petersenstr.30
D-64287 Darmstadt, Germany

H. Urbschat
Fachbereich Physik and ICBM
Carl von Ossietzky Universität Oldenburg
Postbox 2503
D-26111 Oldenburg,Germany

R. B. Griffiths
Department of Physics
Carnegie-Mellon University
Pittsburgh, PA 15213, USA

H.J.Schellnhuber
Potsdam Institute for Climate Impact Research (PIK)
P.O. Box 60 12 03
D-14412 Potsdam, Germany
(Version of June 24, 1997)

A procedure is described for efficiently finding the ground state energy and configuration for a Frenkel-Kontorova model in a periodic potential, consisting of N parabolic segments of identical curvature in each period, through a numerical solution of the convex minimization problem described in the preceding paper. The key elements are the use of subdifferentials to describe the structure of the minimization problem; an intuitive picture of how to solve it, based on motion of quasiparticles; and a fast linear optimization method with a reduced memory requirement. The procedure has been tested for N up to 200.

64.60.Ak,02.60.Pn,03.20.+i,05.45.+b

I. INTRODUCTION

In the preceding paper [1], the problem of finding ground state energies and configurations for a Frenkel-Kontorova model in a periodic potential formed by parabolic segments of identical (positive) curvature, was reduced to that of minimizing a certain convex function over a finite simplex. While various aspects of the corresponding phase diagram in the $N = 2$ case can be worked out in a relatively straightforward manner [2–4], minimizing the convex function for larger values of N represents a non-trivial problem in numerical analysis. The basic reason is that the convex function of interest does not have continuous derivatives, and in the case of an irrational winding number, it possesses a dense set of singularities. Hence standard gradient methods run into difficulties.

The approach we employ is based upon the concepts of subdifferential and subgradient from the theory of convex functions [5], as explained in Sec. II. The algorithm itself, described in detail in Sec. III, is motivated by a physical model involving quasiparticles, Sec. III A. An essential part of the procedure is a standard linear programming procedure which we have simplified and adapted to the problem at hand, App. A, so as to speed it up substantially. As a result, ground states for N on the order of 100 are readily calculated, and larger values of N are accessible with, of course, a longer running time; see Sec. III D.

II. MINIMIZATION USING SUBDIFFERENTIALS

As in part I, with some minor changes in notation, we assume the energy per particle can be written in the form

$$\epsilon = \epsilon_0 + \epsilon_1, \tag{1}$$

where

$$\epsilon_0 = \sum_{j<k} \Delta t_j \Delta t_k \mathcal{G}(\zeta_{kj}), \tag{2}$$

$$\epsilon_1 = \bar{\mathbf{h}} \cdot \boldsymbol{\psi} = -\bar{\boldsymbol{\eta}} \cdot \boldsymbol{\zeta} = -\sum_{i=0}^{N-1} \bar{\eta}_i \zeta_i, \tag{3}$$

with $\bar{h}_0$ equal to zero,

$$\zeta_{kj} = -\zeta_{jk} = \zeta_k - \zeta_j = \sum_{i=j+1}^{k} \psi_i, \tag{4}$$

and

$$\mathcal{G}(\psi) = \mathcal{G}(-\psi) = \mathcal{G}(1-\psi) = \sum_{\nu=-\infty}^{\infty} w g(\frac{\psi+\nu}{w}). \tag{5}$$

The boldface letters denote N-component vectors, for example,

$$\boldsymbol{\zeta} = (\zeta_0, \zeta_1, \ldots \zeta_{N-1}). \tag{6}$$

A constant term independent of $\boldsymbol{\zeta}$ has been omitted from (2), and bars have been added to $\mathbf{h}$ and $\boldsymbol{\eta}$ in (3) to distinguish them from quantities which we shall define later. Note that

$$\sum_{i=0}^{N-1} \bar{\eta}_i = 0 \tag{7}$$

because $\bar{\eta}_i = \bar{h}_{i+1} - \bar{h}_i$, and $\bar{h}_j$ is periodic in j, with period N.

Our task is to find the $\boldsymbol{\zeta}$, or equivalently $\boldsymbol{\psi}$, which minimize ϵ for a given $\bar{\boldsymbol{\eta}}$, or equivalently $\bar{\mathbf{h}}$. The function $\mathcal{G}(\psi)$ is convex on the interval $0 \le \psi \le 1$. If its derivative

$$\mathcal{B}(\psi) = d\mathcal{G}/d\psi = -\mathcal{B}(-\psi) = \mathcal{B}(1+\psi) \tag{8}$$

were a continuous function, the minimum would satisfy the equation:

$$\bar{\boldsymbol{\eta}} = \boldsymbol{\eta} \tag{9}$$

obtained by differentiating (1) , where the components of $\boldsymbol{\eta}$ are given by

$$\eta_k = \sum_{j(\neq k)} \eta_{kj}, \tag{10}$$

$$\eta_{kj} = \Delta t_k \Delta t_j \, \beta_{kj} = -\eta_{jk}, \tag{11}$$

$$\beta_{kj} = \mathcal{B}(\zeta_{kj}) = -\beta_{jk}. \tag{12}$$

But in fact $\mathcal{B}(\psi)$ has lots of discontinuities, see Fig. 1, and therefore we need some way to interpret the (formal) solution (9) in this case. For this purpose it is convenient to employ the concepts of subgradient and subdifferential as defined by Rockafellar [5]. Suppose that $F(\boldsymbol{\zeta})$ is a real-valued function (which need not be convex) defined on some domain in $\mathbb{R}^N$. We shall say that $\boldsymbol{\eta}$ is a *subgradient* of F at the point $\boldsymbol{\zeta} = \bar{\boldsymbol{\zeta}}$ provided

$$F(\boldsymbol{\zeta}) \ge F(\bar{\boldsymbol{\zeta}}) + \boldsymbol{\eta} \cdot (\boldsymbol{\zeta} - \bar{\boldsymbol{\zeta}}) \tag{13}$$

for all $\boldsymbol{\zeta}$ where F is defined. The collection of all $\boldsymbol{\eta}$ values for which this inequality is satisfied for a given $\bar{\boldsymbol{\zeta}}$ is easily shown to be a convex subset of $\mathbb{R}^N$, and is called the *subdifferential* of F at $\bar{\boldsymbol{\zeta}}$, denoted by $\partial F(\boldsymbol{\zeta})$.

Given this definition, it is easy to show that ϵ in (1) has a minimum at $\boldsymbol{\zeta} = \bar{\boldsymbol{\zeta}}$ if and only if $\bar{\boldsymbol{\eta}}$ is an element of $\partial\epsilon_0(\bar{\boldsymbol{\zeta}})$, the subdifferential of ϵ_0 at $\bar{\boldsymbol{\zeta}}$. In addition, the subdifferential of a sum $(F_1 + F_2 + \cdots)$ of convex functions is the sum of the subdifferentials of the individual functions [6], understood as sums of sets of $\mathbb{R}^N$; thus:

$$A + B = \{\boldsymbol{\zeta} + \boldsymbol{\zeta}' : \boldsymbol{\zeta} \in A, \boldsymbol{\zeta}' \in B\}, \tag{14}$$

together with its obvious generalization to the sum of three or more sets.

These observations provide the key for interpreting equations (10) to (12). At some point ψ' where $\mathcal{B}(\psi)$ is discontinuous, the subdifferential of $\mathcal{G}(\psi)$, for ψ in the range $0 \le \psi \le 1$, consists of all points β lying in the interval

$$\mathcal{B}_-(\psi') \le \beta \le \mathcal{B}_+(\psi') \tag{15}$$

where $\mathcal{B}_-(\psi')$ and $\mathcal{B}_+(\psi')$ are the left and right derivatives of $\mathcal{G}(\psi)$ at ψ', that is, the bottom and top of the discontinuity in the graph of $\mathcal{B}$. More generally, for $k > j$ we interpret β_{kj} in (12) as any point in the interval

$$\mathcal{B}_-(\zeta_{kj}) \le \beta_{kj} \le \mathcal{B}_+(\zeta_{kj}), \tag{16}$$

where the lower limit is set equal to $-\infty$ if $\zeta_{kj} = 0$, and the upper limit is $+\infty$ if $\zeta_{kj} = 1$, as a consequence of the constraints

$$\zeta_0 \le \zeta_1 \le \zeta_2 \le \ldots \le \zeta_{N-1} \le \zeta_0 + 1. \tag{17}$$

For $j < k$, we define $\beta_{jk} = -\beta_{kj}$. Of course, if $\mathcal{B}(\psi)$ is continuous at $\psi = \zeta_{kj}$, then β_{kj} is the single point $\mathcal{B}(\zeta_{kj})$.

Consequently, $\partial\epsilon_0(\boldsymbol{\zeta})$ is simply the collection of all $\boldsymbol{\eta}$ obtained using (10), where for each $k > j$, β_{kj} in (12) is allowed to vary over the interval (16), and for $j < k$, $\beta_{jk} = -\beta_{kj}$. Notice that this means that $\eta_{jk} + \eta_{kj}$ is zero, and therefore

$$\sum_{i=0}^{N-1} \eta_i = 0 \tag{18}$$

for any $\boldsymbol{\eta}$ in the subdifferential $\partial\epsilon_0(\boldsymbol{\zeta})$, which corresponds to (7). Note that the β_{kj} are allowed to vary *independently*, aside from the restriction $\beta_{jk} = -\beta_{kj}$. As there are thus $N(N-1)/2$ independent variables, some of which may be constant because they do not correspond to discontinuities of $\mathcal{B}$, $\partial\epsilon_0(\boldsymbol{\zeta})$ is, in general, a fairly complicated polyhedron, of dimension less than or equal to $N-1$, the dimension of the space in $\mathbb{R}^N$ satisfying the constraint (18).

In the case $N = 3$, the subdifferentials $\partial\epsilon_0(\boldsymbol{\zeta})$ are closed sets, either hexagons, lines, or points, depending upon the value of $\boldsymbol{\zeta}$. Some of the lines and hexagons extend to infinity. A hexagon occurs provided

$$\zeta_{10} = \mu_1 w - \nu_1, \quad \zeta_{20} = \mu_2 w - \nu_2, \tag{19}$$

where μ_1, μ_2, ν_1, and ν_2 are integers, in which case ζ_{10} and ζ_{20}, as well as $\zeta_{21} = \zeta_{20} - \zeta_{10}$, are at discontinuities of $\mathcal{B}$. A line occurs when $\mathcal{B}$ is discontinuous at one of the three values ζ_{10}, ζ_{20}, or ζ_{21}, but not at the other two, and $\partial\epsilon_0(\boldsymbol{\zeta})$ is a point if $\mathcal{B}$ is continuous at all three values. If w is irrational, the discontinuities of $\mathcal{B}(\psi)$ are a dense set in ψ, and consequently the subdifferentials of ϵ_0 for different $\boldsymbol{\zeta}$ have no points in common. If w is rational, adjacent hexagons overlap at their common edges and vertices, and each edge and each vertex is itself a subdifferential of ϵ_0 for a range of $\boldsymbol{\zeta}$ values. For both rational and irrational w, the hexagons cover the entire plane satisfying the constraint (18), with the exception, when w is irrational, of a set of zero measure. A similar comment applies to larger values of N, and therefore in numerical studies it suffices to consider the $N-1$ dimensional polyhedra obtained when every ζ_{kj} falls on a discontinuity of $\mathcal{B}$.

It is sometimes helpful to think of the collection of subdifferentials $\partial\epsilon_0(\boldsymbol{\zeta})$ as $\boldsymbol{\zeta}$ varies as generated by placing a set of $N(N-1)/2$ points on the graph of $\mathcal{B}(\psi)$ at positions (ζ_{kj}, β_{kj}). Note that the ζ_{kj} cannot be varied independently, as they are determined by a set of $N-1$ parameters, see (4). However, each of the $N(N-1)/2$ points on the graph can be moved independently in the vertical direction, as long as it is on a discontinuity of $\mathcal{B}$, to form the collection of β_{kj} values which generate the subdifferential for a fixed $\boldsymbol{\zeta}$.

III. NUMERICAL PROCEDURE

A. Introduction

The problem of finding the $\boldsymbol{\zeta}$ which minimizes ϵ, (1) , for a given $\boldsymbol{\eta}$ is equivalent, as noted in Sec. II above, to finding the $\boldsymbol{\zeta}$ such that $\bar{\boldsymbol{\eta}}$ falls in the subdifferential $\partial\epsilon_0(\boldsymbol{\zeta})$. Furthermore, the $N-1$ dimensional polyhedra which arise when all the ζ_{kj} fall at the discontinuities of $\mathcal{B}(\psi)$ fill up the relevant $N-1$ dimensional hyperplane (18) except for a set of measure zero, and as we assume that $\boldsymbol{\eta}$ is only specified with some limited numerical precision, we can in practice limit ourselves to a consideration of such polyhedra.

The general idea of the algorithm is as follows. Starting from some $\boldsymbol{\zeta}$ with all ζ_{kj} at discontinuities of $\mathcal{B}$, test whether the target $\bar{\boldsymbol{\eta}}$ lies inside $\partial\epsilon_0(\boldsymbol{\zeta})$. If it does, the problem has been solved. If it does not, use the information obtained from the test in order to choose a new $\boldsymbol{\zeta}$ closer to the desired value, and repeat the test. The test itself, steps 3 and 5 in the algorithm as summarized below, involves a linear optimization procedure with an execution time which (typically) varies as N^3, which is relatively expensive when N is large. Consequently, the test is preceded in our algorithm by various steps whose aim is to provide, with a relatively small number of operations, a value of $\boldsymbol{\zeta}$ close to the final solution.

To begin with, we replace the actual $\mathcal{B}(\psi)$ with an approximate, piecewise constant function $\mathcal{B}^*(\psi)$ which has discontinuities at the points

$$\psi = \mu w - \nu, \tag{20}$$

where μ and ν are integers, and

$$|\mu| \le M \tag{21}$$

for some finite bound M, which can be increased later if necessary. This is a sensible procedure, because the size of the discontinuities decreases exponentially with $|\mu|$. Between two successive discontinuities ψ' and ψ'', the function $\mathcal{B}^*$ is defined to be a constant lying halfway between $\mathcal{B}_+(\psi')$ and $\mathcal{B}_-(\psi'')$, see Fig. 1. Consequently, the discontinuities of $\mathcal{B}^*$ are somewhat larger than those of the exact $\mathcal{B}$, and (16) is replaced by:

$$\mathcal{B}^*_-(\zeta_{kj}) \le \beta_{kj} \le \mathcal{B}^*_+(\zeta_{kj}). \tag{22}$$

Note that if

$$w = p/q \tag{23}$$

is a rational number, with p and q relatively prime positive integers, the discontinuities of $\mathcal{B}$, (20), are the points

$$\psi = s/q, \tag{24}$$

where s is any integer (and may have factors in common with q). The definition of $\mathcal{B}^*$ is the same as before; though it should be noted that the discontinuity interval of $\mathcal{B}$ at a point (24) is made up of contributions from an infinite number of discontinuities from derivatives of terms on the right side of (5). Of course, if M in (21) is equal to $q-1$ (or larger), $\mathcal{B}^*$ and $\mathcal{B}$ are identical, and step 5 can be eliminated from the algorithm described below.

In order to motivate the initial steps in the algorithm, it is helpful to think of $\zeta_0, \zeta_1, \ldots$ as representing the positions of a set of N quasiparticles located on a circle of unit circumference, Fig. 2, and subjected to two kinds of forces, corresponding to ϵ_0 and ϵ_1, thought of as potential energies. In this picture, $\bar{\eta}_k$ represents an external force exerted on particle k, and η_{kj}, (11), the force which particle k exerts on particle j. The minimization condition (9) can then be interpreted as stating that, for every k, the external force exerted on particle k is equal to the sum η_k of the forces which it exerts on the other particles, which is the same as saying that the net force on particle k is zero. The pair force η_{kj} is constant as long as ζ_{kj} is not at a discontinuity of $\mathcal{B}^*$, while if it is at such a discontinuity, it can take any value, see (11), corresponding to β_{kj} in the range (22). In addition, there is a hard core interaction which prevents two quasiparticles from passing through each other, and ensures that the inequalities (17) are satisfied. Note that there can very well be solutions to the minimization problem in which some of these inequalities are equalities. If, for example, $\zeta_2 = \zeta_3$, then β_{32} can be very large and negative, see the remarks following (16), corresponding to the fact that the hard core allows particle 3 to exert a very large (negative) force on particle 2.

The initial steps of the algorithm consist of a number of horizontal and vertical shifts; the terminology comes from the picture of points on the graph of $\mathcal{B}$, Sec. II. A *horizontal shift* is a change in the positions of the quasiparticles, and thus the ζ_{kj}, with the β_{kj} (and thus the η_{kj}) held fixed, while a *vertical shift* is a change in the set of β_{kj} values with

the quasiparticle positions, and thus the ζ_{kj}, held fixed. In addition, we shall make use of the concept of a *cluster*, which means a collection of quasiparticles, with their labels belonging to an index set J containing $|J|$ members, with the property that the collection is connected by a set of "pair bonds" (kj), k and j members of J, with ζ_{kj} at one of the discontinuities of $\mathcal{B}^*$. For example, if ζ_{21} and ζ_{42} fall on discontinuities of $\mathcal{B}^*$, then it is possible, but not necessary, to define a cluster $J = \{1, 2, 4\}$ of $|J| = 3$ quasiparticles, as in Fig. 2. We shall always think of the entire collection of quasiparticles as divided up among a set of mutually disjoint clusters, where a quasiparticle which does not belong to a larger cluster constitutes its own cluster containing only one element. If all the quasiparticles belong to a single cluster of $|J| = N$ elements, we shall call this a *complete cluster*. In any horizontal shift, the clusters are moved rigidly, in the sense that ζ_{jk} does not change if j and k belong to the same cluster. (This must obviously be the case whenever the cluster is linked together by bonds for which the β_{kj} fall in the interiors of the corresponding discontinuity intervals (22).) Conversely, a vertical shift is always applied to a single cluster.

B. Summary of the Algorithm

The algorithm for finding a minimum consists of the following steps, details of which are given below in Sec. III C.

0. Initialization:

Choose an initial approximate $\mathcal{B}^*$ by, for example, setting $M = 4$ in (21), and some initial values for the ζ_i satisfying (17), with a set of clusters specified (e.g., each quasiparticle might belong to its own cluster).

1. Horizontal shift I:

Calculate a "velocity" for each cluster, and use this to carry out a horizontal shift until for the first time some ζ_{kj} for j and k belonging to different clusters reaches a discontinuity of $\mathcal{B}^*$, in which case we shall say that these two clusters have "collided" to form a temporary combined cluster. Go to step 2.

2. Vertical shift:

Carry out a vertical shift on the temporary combined cluster following the prescription given in (27) below and in the remarks which follow, and apply the test which is described there. If the result of the test is negative, the combined cluster is rejected, the collection of clusters is defined to be the same as it was before the collision, and the algorithm returns to step 1. If the result of the test is positive, the temporary combined cluster becomes permanent, and is considered part of the collection of clusters for the next step in the algorithm. If this cluster is complete, go to step 3; if not, return to step 1.

3. Linear optimization I:

With all the quasiparticles in a single cluster, apply linear optimization, as discussed in Sec. III C below, to produce a vertical shift which maximizes a non-negative parameter λ. If $\lambda \geq 1$, then the target $\bar{\boldsymbol{\eta}}$ is inside the polyhedron $\partial\epsilon_0(\boldsymbol{\zeta})$ associated with the current $\boldsymbol{\zeta}$ in the approximation in which $\mathcal{B}$ has been replaced by $\mathcal{B}^*$; go to step 5. If $\lambda < 1$, then $\bar{\boldsymbol{\eta}}$ is not inside the polyhedron; go to step 4.

4. Horizontal shift II:

Use the β_{kj} resulting from the linear optimization in 3 to divide the collection of quasiparticles into two clusters, which undergo a horizontal shift relative to each other until they collide (as in step 1) to form a new, combined cluster which is a complete cluster. Return to step 3.

5. Linear optimization II:

Repeat the linear optimization step 4, but with each β_{kj} now restricted to the corresponding *exact* interval (16). If, however, ζ_{kj} falls at a point where $\mathcal{B}^*$, unlike $\mathcal{B}$, has no discontinuity, then the corresponding β_{kj} is placed at the center of the corresponding discontinuity of $\mathcal{B}$, and is treated as a constant, not a variable, during the linear optimization. If the optimization yields $\lambda \geq 1$, the current $\boldsymbol{\zeta}$ is the desired solution to the minimization problem, and the algorithm stops. If λ is less than 1, $\mathcal{B}^*$ is replaced by another approximation to $\mathcal{B}$ constructed in the same way, but using a larger value of M in (21). The current $\boldsymbol{\zeta}$ values are changed by very small amounts so that none of the ζ_{kj} fall at discontinuities of the new $\mathcal{B}^*$, and the algorithm returns to step 1.

C. Details of the Algorithm

The explanations given below are numbered in the same way as the steps in the preceding summary.

1. Given a set of η_{kj} values, the net force on the k'th quasiparticle is

$$\bar{\eta}_k - \eta_k = \bar{\eta}_k - \sum_{j(\neq k)} \eta_{kj}. \tag{25}$$

Were the force given by a continuous function, it would be possible to find the energy minimum by assigning to each quasiparticle a velocity proportional to the force acting on it, and then solving the resulting dynamics. What is actually done in the algorithm is to assign to each cluster a velocity given by the total force acting on all the quasiparticles in the cluster divided by the number of particles in the cluster, which is the average force per particle:

$$v_J = (1/|J|)\sum_{k\in J}(\bar{\eta}_k - \eta_k). \tag{26}$$

It is only the relative cluster velocities which are of interest in determining the horizontal shift; adding the same constant to every v_J will make no difference, and one can arrange (for example) that the cluster containing ζ_0 remains fixed. The clusters are then shifted by amounts proportional to their respective velocities until the first "collision" occurs, in the sense that ζ_{kj} for k in one cluster and j in another reaches a discontinuity of $\mathcal{B}^*$.

2. Once the temporary, combined cluster J_c has been formed, a vertical shift is applied to the η_{kj} for k and j in J_c. This is done by first calculating a preliminary value for the shift of the η_{kj} or β_{kj} values from the formula

$$\delta\eta_{kj} = \Delta t_k \Delta t_j \, \delta\beta_{kj} = [(\bar{\eta}_k - \eta_k) - (\bar{\eta}_j - \eta_j)]/|J_c|. \tag{27}$$

The motivation for this choice is the following. If all the quasiparticles were in a single cluster, $|J_c| = N$, the change (27) would result in a new set of pair forces

$$\eta'_{kj} = \Delta t_k \Delta t_j \, \beta'_{kj} = \eta_{kj} + \delta\eta_{kj} \tag{28}$$

with the property that

$$\bar{\eta}_k = \eta'_k = \sum_{j(\neq k)} \eta'_{kj}, \tag{29}$$

that is, one would have solved the minimization problem. With $|J_c| < N$, the result would, instead, be to make the difference $\bar{\eta}_k - \eta'_k$, the sum of the forces acting on quasiparticle k, independent of k for all k in J_c, and to minimize

$$\sum_{k\in J_c} (\bar{\eta}_k - \eta'_k)^2 \tag{30}$$

as much as is possible by changing only the pair interactions η_{kj} inside the cluster J_c.

However, formula (27) does not take account of the possibility that the β'_{kj} in (28) might lie outside the interval (22) determined by $\mathcal{B}^*$. When this is the case, the new β'_{kj} is placed at whichever end of the discontinuity interval lies closest to the value given by (28). The test for rejecting or retaining the combined cluster J_c is then the following. If for each of the pairs k and j for which k belongs to one of the clusters involved in the collision and j to the other, the new β'_{kj} is at one of the ends of the interval (22), the combined cluster J_c is rejected, whereas if at least one of these values falls in the interior of the corresponding interval, J_c is accepted. Note that whether the cluster J_c is accepted or rejected, the new values of β'_{kj}, and thus the corresponding η'_{kj}, produced in the vertical shift are retained when going on to the next step of the algorithm, which is either step 1 or, in the case in which J_c is accepted and $|J_c| = N$, step 3.

The algorithm would still function correctly if a combined cluster were never rejected. However, this would mean having to apply linear optimization, step 3, more often, and would result in a slower computation. The process of allowing clusters to move relative to each other past discontinuities which represent relatively small changes compared to the large forces representing a situation "far from equilibrium" helps to achieve a better preliminary value of $\boldsymbol{\zeta}$ before going on to step 3.

3, 4. The linear optimization step is basically a test to see whether the target $\bar{\boldsymbol{\eta}}$ lies inside the polyhedron representing $\partial\epsilon_0(\boldsymbol{\zeta})$ in the approximation in which $\mathcal{B}$ is replaced by $\mathcal{B}^*$. The idea is to begin at a particular vertex $\boldsymbol{\eta}^c$ of the polyhedron, Fig. 3, and draw a straight line from $\boldsymbol{\eta}^c$ to the target $\bar{\boldsymbol{\eta}}$. Points along this line are of the form

$$\boldsymbol{\eta} = \boldsymbol{\eta}^c + \lambda(\bar{\boldsymbol{\eta}} - \boldsymbol{\eta}^c), \tag{31}$$

where λ is a number between 0 and 1. The linear optimization procedure, the details of which are given in the appendix, determines the largest value of λ for which a point of the form (31) lies inside or on the boundary of the polyhedron. If this value is less than 1, as in Fig. 3, the target lies outside the polyhedron, and the point (31) determined by the maximum value of λ specifies a facet of the polyhedron lying in the direction of the target, as viewed from the starting vertex $\boldsymbol{\eta}^c$. This facet is generated by letting $(N-2)$ of the β_{kj} vary over their entire discontinuity

intervals, while the remaining β_{kj} are fixed either at the top or at the bottom of their discontinuity intervals. The ζ_{kj} corresponding to the former are "rigid" in the sense that they cannot be altered by a horizontal shift (which, by definition, must leave the β_{kj} unchanged), and one can identify two clusters of quasiparticles, each one connected by such rigid bonds.

Once these two clusters have been identified, they can be shifted relative to each other, in a direction which is obvious, until they collide at the first discontinuity of $\mathcal{B}^*$. This collision results in a new, complete cluster, and the corresponding $\partial\epsilon_0(\boldsymbol{\zeta})$ is a polyhedron adjacent to the one considered earlier, and shares with it the facet which was identified in the previous linear optimization step.

Note that this new cluster is accepted without carrying out the test used in step 2 of the algorithm. Also, in the unlikely event that the maximum λ corresponds to the intersection of two or more facets of the polyhedron, the actual optimization algorithm described in the appendix will, in effect, "choose" one of these facets, and thus the polyhedron adjacent to it in the direction of the target $\bar{\boldsymbol{\eta}}$.

5. If the optimization carried out in step 3 yields $\lambda \geq 1$, the target $\bar{\boldsymbol{\eta}}$ lies inside the polyhedron generated by the discontinuities of $\mathcal{B}^*$, but it may or may not lie inside the corresponding polyhedron generated by restricting the β_{kj} to lie in the exact interval (16) for the corresponding discontinuity. To test whether this is the case, one repeats the linear optimization technique of step 3, but now starting with each β_{kj} at its *exact* maximum possible value, and constrained to be greater than or equal to its *exact* minimum possible value, with the exception of those β_{kj} for which ζ_{kj} does not fall at a discontinuity of $\mathcal{B}^*$, which are assigned fixed values at the center of the appropriate (exact) discontinuity intervals of $\mathcal{B}$. One could, of course, make *all* of the β_{kj} variable during the linear optimization process. However, as the discontinuity intervals in $\mathcal{B}$ which are not in $\mathcal{B}^*$ are, by construction, relatively small, the main effect of using a larger set of variables would be to slow down the linear optimization without much hope of actually finding a solution with $\lambda \geq 1$ when the restricted search yields one with $\lambda < 1$. Note that if such a restriction does result in overlooking a $\lambda \geq 1$ solution, this solution, or one equivalent to it, will nevertheless be found later when the number of discontinuities of $\mathcal{B}^*$ is increased.

If the maximum value of λ obtained by using linear optimization with the exact discontinuity intervals of $\mathcal{B}$ is still greater than or equal to 1, then the current $\boldsymbol{\zeta}$, and thus the current set of ζ_{kj}, represents an actual solution to the minimization problem, and this does not depend upon the approximations used in constructing $\mathcal{B}^*$, because the resulting β_{kj} values all fall within the range where $\mathcal{B}^*$ is identical to $\mathcal{B}$.

If, on the other hand, one finds that λ is less than 1, this means that the current $\boldsymbol{\zeta}$ is not a solution to the true minimization problem; instead, it is as good as one can do using the approximate $\mathcal{B}^*$. To do better, it is necessary to increase the number of discontinuities. Our procedure at this point is to throw away all the information associated with the β_{kj} values obtained in the immediately preceding step of linear optimization, and simply start over again at step 1 using the current $\boldsymbol{\zeta}$. One might be able to improve the algorithm in this respect, but since the initial steps of the algorithm are relatively fast, it does not seem likely that one would obtain a significant increase in speed.

D. Implementation and Performance

The program we constructed to implement the algorithm described above was tested in the following way. We chose a winding number equal to the inverse golden mean (0.618...) and a value of κ, see [1], of 0.6, resulting in a set of 60 pairs (ψ and $1-\psi$) of discontinuities of $\mathcal{B}$ in the interval $0 \leq \psi \leq 1$ with a magnitude greater than a resolution of 10^{-20}. (Some tests used alternative values for κ, 0.1, 0.5, and 1.0, for which there are 146, 66, and 47 pairs of discontinuities, respectively, exceeding this resolution.) The parabolas were assumed to be equally spaced, with Δt_l independent of l. Then we employed the following "inverse strategy". With N fixed, random values of ζ_j, lying on the full set of discontinuities of $\mathcal{B}$ were chosen, subject to the constraints (17), and values η_{kj} inside the discontinuity intervals were also chosen randomly, thus defining—see (10), (9), and (3)—$\bar{\boldsymbol{\eta}}$ for a model of N parabolas with the solution to its energy minimization problem already known. The algorithm was then applied to this model starting at the initialization step 0, with a (different) random collection of ζ_i, and a choice of M (the number of pairs of discontinuities in the approximate $\mathcal{B}^*$) to search for the correct solution.

Note that the running time increases linearly with M. But since as M increases, the size of the discontinuities in $\mathcal{B}^*$ is decreasing, the probability that a random choice of $\bar{\boldsymbol{\eta}}$ will actually require a larger value of M goes to zero exponentially with increasing M. We found that using an initial value of $M = 2$ when N is small saves a lot of running time, and in almost all cases $M = 10$ was sufficient to find a ground state with N up to 100.

To determine the N dependence of the running time, we generated and timed 10 distinct potentials for each N in an increasing series up to $N = 115$. Using an HP 9000 model 735 workstation with 64 MB of RAM and a CPU with 20 MFLOPs, the average time in seconds required to find a solution was approximately $10^{-5}N^4$, or a quarter of an hour for $N = 100$. The time required for linear optimization varies as N^3, but as N becomes larger, "quasiparticle

dynamics" takes up a larger fraction of the time: 60-70% for $N = 100$. The algorithm found the correct ground state in particular cases for N as large as 200.

ACKNOWLEDGMENTS

We would like to thank S. Aubry, P. Delaly, A. Hamm, R. S. MacKay and P. Rujan for useful discussions. This work was supported by the Deutsche Forschungsgemeinschaft (Bonn, Germany).

APPENDIX A: LINEAR OPTIMIZATION

The linear optimization procedure used in steps 3 and 5 of the algorithm functions in the following way. Written out in terms of components, Eq.(31) has the form:

$$\eta_k = \eta_k^c + \lambda(\bar{\eta}_k - \eta_k^c) = \sum_{j \neq k} \Delta t_k \Delta t_j \beta_{kj} \tag{A1}$$

for $k = 1, 2, \ldots, N-1$. The equation for $k = 0$ can be omitted because of the constraints (7) and (18). In turn, the β_{kj} for $k > j$ can be written as

$$\beta_{kj} = \mathcal{B}_+^*(\zeta_{kj}) + x_{kj}[\mathcal{B}_-^*(\zeta_{kj}) - \mathcal{B}_+^*(\zeta_{kj})], \tag{A2}$$

where the $N(N-1)/2$ variables x_{kj} take values on the closed interval

$$0 \leq x_{kj} \leq 1. \tag{A3}$$

In step 5 of the algorithm, $\mathcal{B}^*$ in (A2) should be replaced with the exact function $\mathcal{B}$. The vertex $\boldsymbol{\eta}^c$ of the polyhedron is defined as the value of $\boldsymbol{\eta}$ when $\lambda = 0$, and is obtained by setting all the x_{kj} in (A2) equal to zero, and inserting the resulting β_{kj} in the right side of (A1). It is, thus, a known quantity, as is also the target $\bar{\boldsymbol{\eta}}$. By contrast, the x_{kj} and λ are considered as variables subject to the $N-1$ equalities obtained by inserting (A2) in (A1), and the inequalities (A3), along with $\lambda \geq 0$. If we define the objective function to be equal to λ, maximizing λ subject to these constraints becomes a standard problem in the theory of linear optimization. For a compact but clear description, see [7]. The usual approach is to replace the second set of inequalities in (A3) by the requirement that the "slack" variables

$$y_{kj} = 1 - x_{kj} \tag{A4}$$

be non-negative. However, in order to minimize the number of variables, we have modified the formulation in [7], as discussed below, so that at any point in the calculation, either x_{kj} or y_{kj}, but not both, appears as a variable in the tableau.

The first task is to construct a tableau in restricted normal form, in which the $N-1$ equalities (A1), expressed in terms of the x_{kj} using (A2), are transformed into expressions in which $N-1$ of the x_{kj} variables are expressed as linear functions of the remaining x's and λ. To see how this is done, note that since the $k = 0$ equation is missing from the set (A1), x_{k0} occurs only in the k'th equation, and in none of the others. Therefore, if, for each $k > 0$, the coefficient of x_{k0} in (A2) is non-zero, we can rewrite the $N-1$ equalities in the form

$$x_{k0} = \ldots \tag{A5}$$

for $k = 1, 2, \ldots, N-1$, with no x_{j0} appearing anywhere on the right side of any of these equations.

It may, however, happen that the coefficient of some x_{k0} in (A2) vanishes, because $\mathcal{B}^*(\psi)$ does not have a discontinuity at $\psi = \zeta_{k0}$. In this case the following strategy can be employed. Construct a graph in which the N quasiparticles are vertices, and they are connected together in one cluster using $N-1$ edges (k, j) chosen so that for each edge the coefficient of x_{kj} in (A2) does not vanish. Such a graph is a tree with no closed loops, because a connected graph of N vertices which includes a loop will have at least N edges. One then chooses some vertex m which has only one edge connecting it to another vertex n, and solves the equation (A1) with $k = m$ for x_{mn} (or x_{nm}) in terms of the other x's. After this, eliminate vertex m and the edge (mn) from the graph, and repeat the process. At each stage one finds (it is useful to work out an example) that the only x's appearing on the right side of the equation either do not correspond to edges of the original graph, or else to edges which have already been eliminated. The latter, however, can be expressed (recursively) as functions of the x's corresponding to edges which were not present in the

original graph, thus leading to a set of $N-1$ equalities of a form similar to (A5). Note that the x_{kj} whose coefficients are zero in (A2) can be completely eliminated in constructing the linear optimization tableau, as they play no role.

Once the tableau has been constructed for the restricted normal form, the optimization is carried out as indicated in [7], with the following difference. When considering increasing the variable associated with a particular column, it is necessary to take account of both positive and negative entries in the column in order to test whether one of the left x_{kj} will reach either the upper or lower limit in (A3). If the choice is to set a left variable x_{kj} equal to 1, it is replaced as a right variable by the corresponding y_{kj}, which is 0, and the tableau is appropriately transformed.

---

[1] R.B.Griffiths, H.J.Schellnhuber, H.Urbschat (preceding paper).
[2] R. B. Griffiths, H. J. Schellnhuber and H. Urbschat, Phys.Rev.Lett. 65, 2551 (1990).
[3] P. Delaly, Ph.D. Thesis, Carnegie-Mellon University, 1995 (unpublished).
[4] H. C. Kao, S.-C. Lee, and W.-J. Tzeng, Preprint (solv-int/9607001).
[5] R. T. Rockafellar, *Convex Analysis* (Princeton University Press, Princeton, N. J., 1970) Part V.
[6] See p. 223 of [5].
[7] W. H. Press, S. A. Teukolsky, W. T. Vetterling, and B. P. Flannery, *Numerical Recipes in C* (Cambridge University Press, Cambridge, U.K., 1988), Sec. 10.8.

FIG. 1. The exact $\mathcal{B}(\psi)$ (solid lines) for a winding number equal to the inverse golden mean (.618...) and $\kappa = 0.1$ is shown by solid lines, and the approximation $\mathcal{B}^*(\psi)$, which retains only the largest discontinuities (see text) by dashed lines.

FIG. 2. An example of $N = 6$ quasiparticles lying on a circle of unit circumference and partially coupled to a cluster with index set $J = \{1, 2, 4\}$.

FIG. 3. Schematic representation of the linear optimization procedure, see (31). Points $\boldsymbol{\eta}$ with λ less than 0.6 lie inside the polyhedron (in this case a polygon), so that the target $\bar{\boldsymbol{\eta}}$ lies outside it, and the open circle corresponding to the maximum value of λ indicates the starting point for the next step of the algorithm.

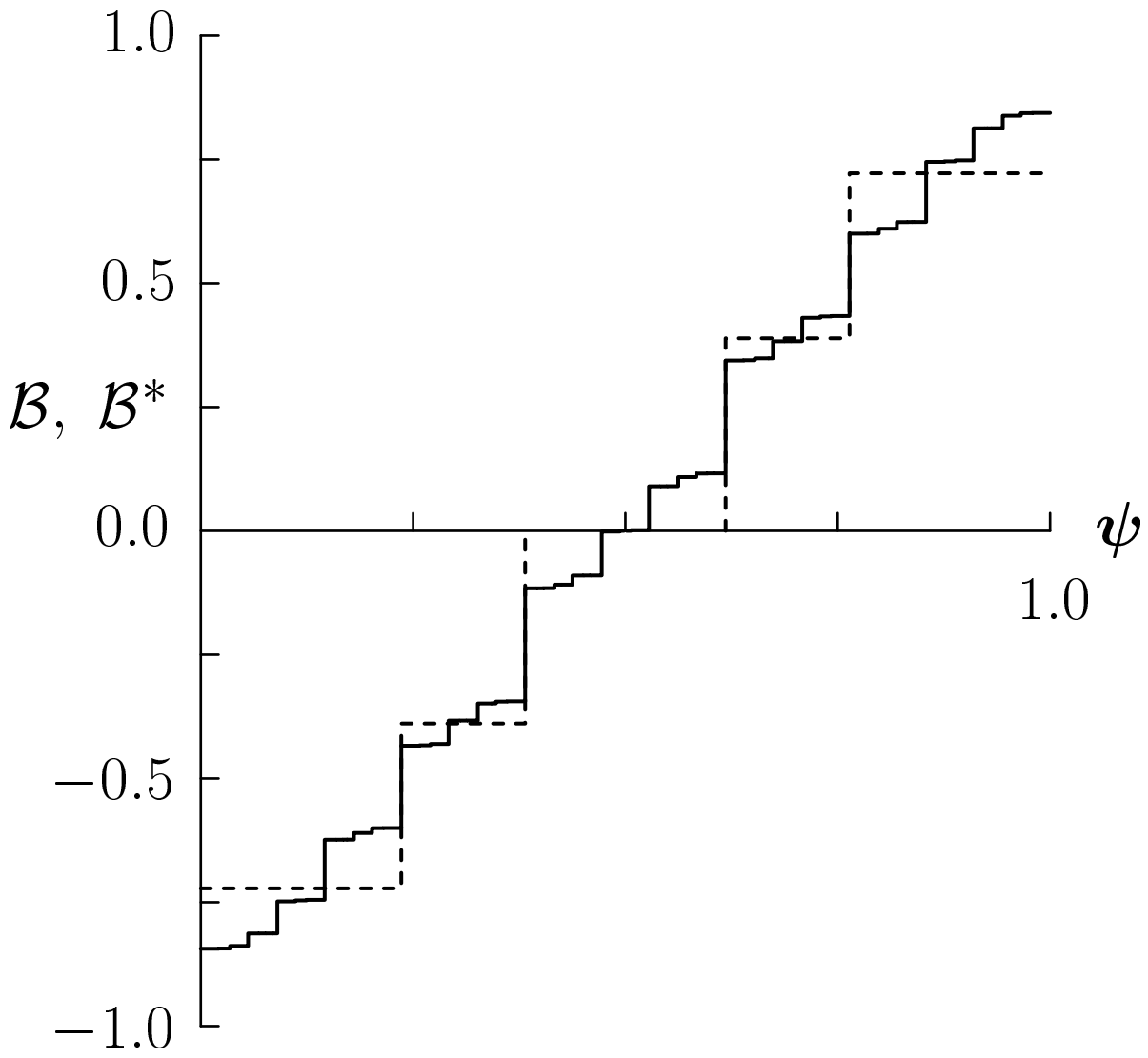
1.0
0.5
$\mathcal{B},\ \mathcal{B}^*$
0.0
ψ
1.0
-0.5
-1.0

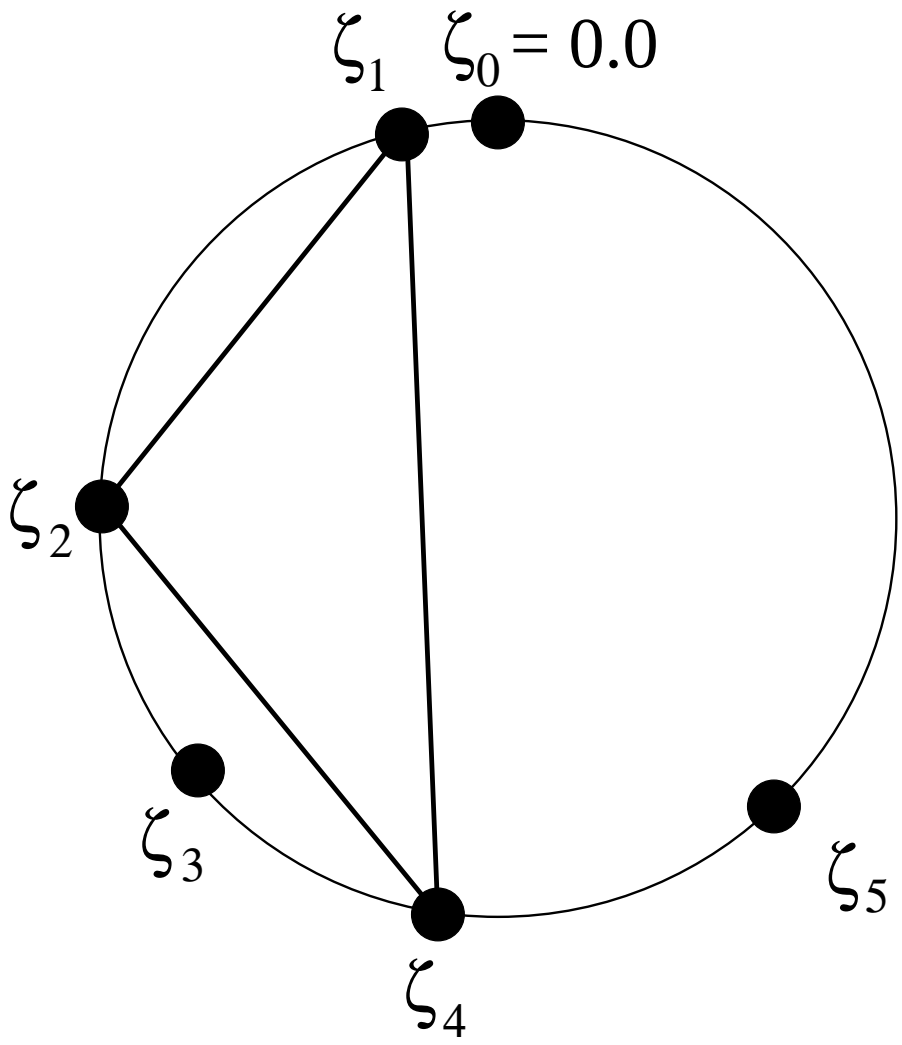
ζ_1
$\zeta_0 = 0.0$
ζ_2
ζ_3
ζ_4
ζ_5

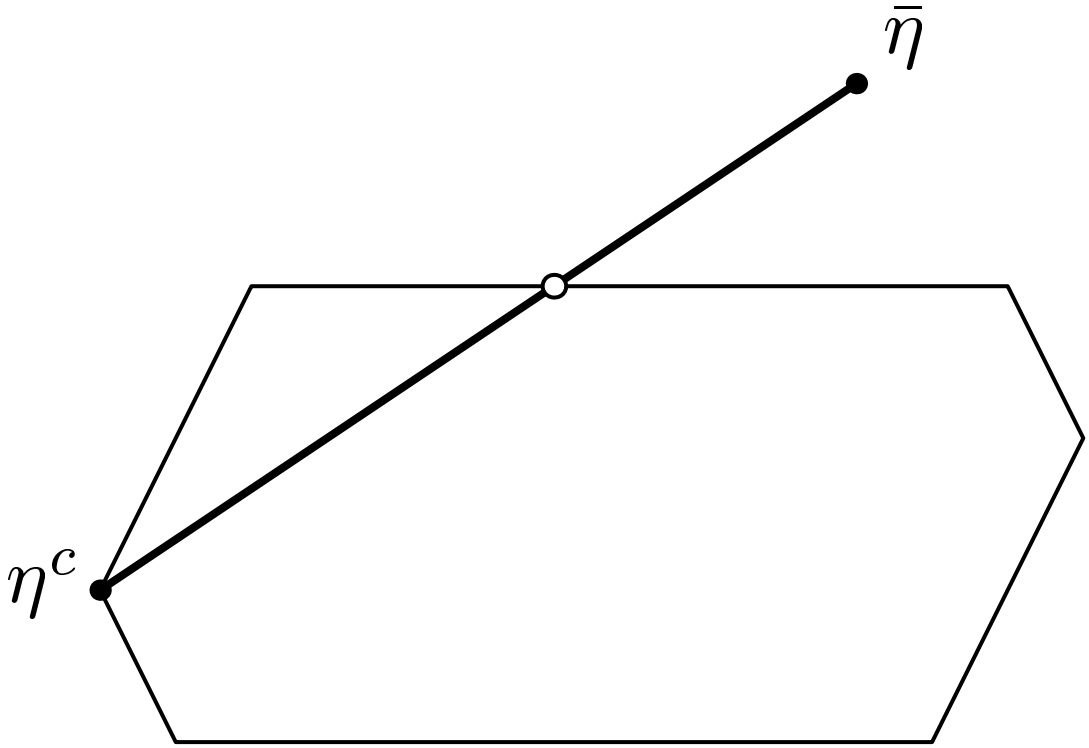
$\bar{\eta}$
η^c